Electrical and thermal conductivities and Seebeck coefficient of liquid copper-bismuth alloys

Karim Khalouk, Cheikh Chaib, Jean-Georges Gasser

Electrical and thermal conductivities and Seebeck coefficient of liquid copper-bismuth alloys

Journal:	*Philosophical Magazine & Philosophical Magazine Letters*
Manuscript ID:	TPHM-08-Aug-0273.R1
Journal Selection:	Philosophical Magazine
Date Submitted by the Author:	23-Oct-2008
Complete List of Authors:	KHALOUK, Karim; Université Paul Verlaine - Metz, Laboratoire de Physique des Milieux Denses CHAIB, Cheikh; Faculté des Sciences Université Mohamed 1er, Laboratoire de Physique du Solide GASSER, Jean-Georges; Université Paul Verlaine - Metz, Laboratoire de Physique des Milieux Denses
Keywords:	electronic transport, experimental, liquid alloys, resistivity, theoretical, thermal transport, thermoelectric power
Keywords (user supplied):	Faber-Ziman theory, muffin tin potential, t matrix

Electrical and thermal conductivities and Seebeck coefficient of liquid copper-bismuth alloys

K. Khalouk[a], C. Chaïb[a,b] and J.G. Gasser[a,*1]

[a] Laboratoire de Physique des Milieux Denses
Université Paul Verlaine - Metz
1 Bd Arago, 57078 Metz cedex 03, France
[b] Laboratoire de Physique du Solide, Faculté des Sciences,
Université Mohamed 1er, 60000 Oujda, Morocco.

Keywords Liquid metals, liquid alloys, resistivity, thermopower, thermal conductivity, phase shifts, muffin tin potential, t matrix, Faber-Ziman theory.

Abstract

The electrical resistivity and the absolute thermoelectric power of the liquid Cu_x-$Bi_{(1-x)}$ system have been measured over the whole composition range from the liquidus to 1100°C. The thermal conductivity is deduced from measurements of these two properties. The experimental results are interpreted and discussed in term of the extended Faber-Ziman formula using the t-matrix formalism with hard-sphere structure factors. The concentration and energy dependence of the phase shifts have been taken into account for a complete conductivity and thermopower calculation.

[1] Corresponding author ***Prof. Jean-Georges GASSER*** **L**aboratoire de **P**hysique des **Mi**lieux **D**enses (**L.P.M.D.**) Université Paul Verlaine – Metz. 1 Bd Dominique François ARAGO 57070 METZ (FRANCE)
Tél: (33) 3 87 31 58 59 Fax: (33) 3 87 31 58 84 Email: gasser@univ-metz.fr

I Introduction

The aim of this paper is to report on the electrical resistivity and on the **A**bsolute **T**hermoelectric **P**ower (**ATP**) measurements of liquid Cu_x-$Bi_{(1-x)}$ alloys between the melting point and 1100°C and over the whole concentration range (by ten atomic per cent steps). The thermal conductivity due to electrons is linked by an exact relation to different electronic transport coefficient like the electrical resistivity and the thermopower (called indifferently Absolute Thermoelectric Power, ATP or thermopower). Its simplified relation is known as the Wiedemann-Franz law. These relations have been presented in solid state physics textbooks by Ziman [1,2] and by Barnard [3] in the thermoelectric power bible "Thermoelectricity in metals and alloys". We prefer the more tractable presentation by Young [4] discussed by Sar et al. [5]. To our knowledge no thermoelectric power measurements have been published. Only Takeuchi et al. [6] made some measurements by a less accurate "electrodeless technique" (five concentrations) on the resistivity of this system. The experimental method has been described by Sar [5], the theoretical formula and the main steps allowing the computation for pure metals and alloys have been presented by Chaïb et al. [7]. Our experimental results are presented and compared with the theoretical calculations.

II Theory

* Electronic transport properties

The pure metal Ziman formulation [8] of the electrical resistivity was extended to binary alloys by Faber-Ziman [9]. The resistivity of a liquid alloy can be written:

$$\rho = \frac{3\pi m^2 \Omega_o}{e^2 \hbar^3 k_F^2} \int_o^1 c_1 |t_1|^2 [1 - c_1 + c_1 a_{11}(q)] + c_2 |t_2|^2 [1 - c_2 + c_2 a_{22}(q)] + c_1 c_2 (t_1^* t_2 + t_1 t_2^*)[a_{12}(q) - 1] 4 (\frac{q}{2k_F})^3 d(\frac{q}{2k_F}) \quad (1)$$

$a_{ij}(q)$ are the partial structure factors, Ω_o the atomic volume of the alloy, k_F the Fermi wave vector, $t(q,E_F)$ the one particle t matrix describing the amplitude for electron-ion scattering at

Fermi energy E_F and momentum transfer q. We used the Faber-Ziman [10] partial structure factors $a_{ij}(q)$. These functions are calculated with the Ashcroft and Langreth [11] hard sphere model. The hard sphere diameters are obtained as in [7] and are held constant over the whole concentration range at constant temperature. It is well known that bismuth is one of the polyvalent elements which present a shoulder on the high angle side of the main peak, like germanium. The shoulder is the most important near the melting point and vanishes with temperature. Isherwood and Orton [12] measured the structure factor from 303 to 652°C . It is interesting to observe how the shoulder vanishes as the temperature is increased. It quasi disappeared at 950°C, the highest temperature tabulated in Waseda's book [13]. Our calculations are made at 1100°C, i.e. 830°C above the melting point. It is possible to consider that at this temperature the shoulder completely disappeared.

The thermopower can be written:

$$S = \frac{\pi^2 k_B^2 T_K}{3|e|E_F}\chi \quad \text{where} \quad \chi = \left[\frac{\partial \ln \rho}{\partial \ln E}\right]_{E_F} \tag{2}$$

where k_B is the Boltzman constant, T_K the temperature in Kelvin and χ the dimensionless thermoelectric parameter. The thermopower is the logarithmic derivative of the resistivity. The thermoelectric parameter χ can be expressed as : $\chi = 3 - 2\alpha - \beta/2$. The expression of α and β can be found in ref. [7]. The energy dependent term β is difficult to calculate and is generally neglected. In this case we obtain a energy independent calculation of the thermopower. The result of this calculation will be written $\mathbf{S_{local}}$. We have calculated the thermoelectric power by the numerical derivation of the resistivity as a function of energy for alloys. Thus it includes the energy-dependent term, which is very difficult to calculate analytically. The result of the full calculation will be written **S**. The thermal conductivity due to electrons is linked to the electrical resistivity and to the Seebeck coefficient by equation 3a. A simplified expression is called the Wiedemann-Franz law (equation 3b). More details are given in [14].

3a) $\lambda = \frac{(L_0 - S^2)T_k}{\rho}$ 3b) $\lambda \approx \frac{L_0}{\rho} T_K = L_0 T_K \sigma$

L_0 is the Summerfield value of the Lorenz number ($2.45 \times 10^{-8} W\Omega.K^{-2}$), $\sigma = 1/\rho$ is the electrical conductivity. Recently, a review article on the calculation of electron transport properties in the framework of the extended Faber-Ziman theory has been published by Gasser [15].

* Muffin tin potential construction

The construction of the liquid copper and bismuth potentials is based on the superposition of neutral atomic charge densities and potentials following the well known Mattheiss prescription [16] established for solids and described for liquids in [7]. We use the Mukhopadhyay et al. [17] approach in the muffin tin potential construction in order to take care of the specific neighbour sites arrangement in the liquid. The exchange correlation part of the liquid potential has been expressed using Slater exchange approximation [18] and depends simply on the total electronic charge density at any distances r.

* Phase-shifts and Fermi energy

The phase shifts entering in the expression of the electronic properties are calculated from a muffin-tin potential as described in [7]. Once the phase shifts are given as function of energy, we have to estimate the Fermi energy which is the most important parameter in calculations of electronic transport properties. Esposito et al. [19] proposed a consistent method to determine E_F. This method has been described and used in [7].

III Experimental method

The experimental results were obtained using an automated device which measures jointly the electrical resistivity and the absolute thermopower. This method has been completely described by Sar et al.[5]. It combines a measurement of the electrical resistivity using a four-point probe technique, and a measurement of the absolute thermoelectric power employing a small ΔT method. The liquid metal is contained in a fused silica cell provided with sealed tungsten (W) and W-26 wt % Re electrodes. The geometrical constant of the cell was determined by measuring the well known resistivity of triple-distilled mercury at room temperature [20]. The thermoelectric power of tungsten and W-26 wt% Re were previously calibrated with a 'platinum 67' wire. Its absolute thermoelectric power was given by Roberts [21]. The error in the final results is estimated to be no more than ± 0.4μΩ.cm for the resistivity and ± 0.5 μV/°C for the thermoelectric power in the whole temperature range studied.

IV Experimental results and discussion

1 Pure bismuth

We represent the resistivity and the thermopower of pure bismuth respectively on figure 1 and 2. On figure 1 we observe a nearly linear temperature dependence of the resistivity of liquid bismuth. The difference with earlier measurements is lower than 0.7%. On figure 2 we observe a negative thermopower decreasing non linearly with temperature. The difference with earlier measurements is lower than 0.1 $\mu V / K$. Data of the present calculations with the Slater exchange are summarised in table 1. The energy dependence of the electrical resistivity ρ(E) and of the thermopower S(E) are plotted in figure 3 and 4 respectively using the $\eta_l(E)$ phase shift (figure 5). Once E_F is located by the filling of the band procedure, the phase shifts and their energy dependence at E_F can be calculated in order to evaluate the resistivity and the thermopower of the liquid metals. Furthermore, in case of the alloys we have taken into

account the concentration energy dependence of the phase shifts in calculating the corresponding resistivity.

We have calculated the phase shifts as function of energy for pure bismuth (figure 5). To obtain bismuth Fermi energy we considered the case in which the band $6s^2$ and $6p^3$ would be separated as it was observed by Indlekofer [22,23] by experimental determination of the density of states through XPS and UPS measurements. The density of states obtained by ab initio numerical calculations by Hafner et al. [24] leads to the same conclusions. The experimental, free electron and calculated density of states are represented and compared on figure 6. It can be objected that the experimental Hall effect of liquid bismuth measured by different authors [25,26] and collected in Lee and Lichter review article [27] leads to a very high number of free electrons (near 8) which is obviously not physical. It is thus not possible to consider that free electron formalism is adapted to explain the Hall coefficient of liquid bismuth. Indeed, Enderby [28] introduces a correction corresponding to the Mott squared g factor. Ballentine and Huberman [29] developed a theory of Hall Effect in liquid metals. They introduce a "skew scattering" due to spin orbit coupling. Their calculation is made with numerical values of phase shifts corresponding to 5 free conduction electrons, not to 3 as expected from DOS measurements and Hafner's [24] calculations. It is necessary to recall that the phase shifts are strongly energy dependent. Thus the only conclusion is that we do not have a clear theoretical situation allowing interpreting the Hall coefficient of heavy liquid metals. The calculated value must result from a combination of energy dependent phase shifts, of spin orbit coupling and of density of states correction all at the correct Fermi energy. We have thus taken the Fermi energy in both hypothesis (Z=3 and Z=5), the first one being physically better justified.

The resistivity versus energy is plotted in figure 3. For bismuth, the resistivity calculated using the valence 3 shows an excellent agreement with the experiment ($\rho_{\exp} = 163.6\ \mu\Omega.cm$ compared to $\rho_{cal} = 161.9\ \mu\Omega.cm$) at 950°C. The calculations made with the valence 5 leads to a too low resistivity (it represents nearly 46 % of the experimental value). The local calculation of the thermopower versus energy (energy dependent term β neglected) gives a non physical high positive thermopower (upper curve in figure 4). The full non local energy dependent calculation gives a negative thermopower (as experimentally measured). In this case we can

obtain the best agreement, contrary to the resistivity, by using the valence 5. However, we observe that whatever the Fermi energy is, the complete calculations of the thermoelectric power always remain lower then the experiment. For pure liquid copper, the calculations have been made by Chaïb et al. [7].

2 Liquid alloys

Our resistivity and thermopower measurements versus temperature are shown in figures 7 and 8 respectively at different concentrations. The deduced thermal conductivity is plotted in figure 9. On figure 8 and 9 a change of scale has been used for pure copper. We determined the least mean square coefficients of the second order polynomial for resistivity (table 2) and thermopower (table 3) for a better description of the experiment. The temperature dependence of the resistivity seems nearly linear for all the concentrations and the slope is always positive as can be observed directly on curve 7 and by the small second order term in table 2. The resistivity increases with bismuth concentrations (fig 7) when the thermoelectric power decreases rapidly from a high positive value for pure copper to a negative one for bismuth (fig 8). The thermal conductivity is deduced from the knowledge of the electrical resistivity and the thermoelectric power following the formula 3b. Figure 9 shows the thermal conductivity as function of temperature. The thermal conductivity is a linear function of temperature and the slope is positive for all compositions. The scale is not the same for pure copper than for the other alloys. The thermal conductivity increases when adding copper.

The resistivity as a function of the atomic concentration of bismuth (at 1100°C) is represented on figure 10 and is compared to the experimental values of Takeuchi [6]. A good agreement exists between our results and those of Takeuchi (the difference is less then 1μΩ.cm) except for the 80 at.% concentration of copper where we can notice an important difference of about

14μΩ.cm. Figure 11 shows the thermoelectric power as a function of concentration at 1100°C. It decreases rapidly when adding a small concentration of bismuth. Above 10 at.% of bismuth a very small decrease of thermoelectric power with concentration is then observed. The thermal conductivity as function of bismuth concentration is plotted on figure 12. The accuracy is not so good for pure copper since the resistivity is poorly described for pure copper.

The theoretical interpretation of the resistivity and of the thermoelectric power was made according to the Faber-Ziman formula using 3 valence electrons for bismuth following the conclusions for pure bismuth. The calculated results represent very well the experimental curve for resistivity (figure 10), thermopower (figure 11) and thermal conductivity (figure 12). It can be clearly concluded that it is not possible to neglect the energy dependence in the thermopower calculation. The local term gives a large positive value, $25\,\mu V/K$ above the experimental one. Using the full calculation of thermopower, a reasonable difference is still observed between calculation and experiment for pure bismuth and on the whole bismuth riche side part of the phase diagram. However the calculated curve follows the shape of the experimental one and is almost parallel to it; The maximum difference between these two curves is of about 6μV°/K. The thermal conductivity deduced from the experimental resistivity and thermopower is represented as function of concentration on figure 12 and is compared to our Faber-Ziman calculation. The results are very good except for pure copper.

VI Conclusion

We have presented new experimental results of resistivity and thermoelectric power of the copper-bismuth liquid system. Thermal conductivity was deduced using equation (3a). To our knowledge, no thermoelectric power measurement of this system has been made before. Our resistivity measurements allowed us to confirm and complete Takeuchi's results. The theoretical interpretation was made in a very satisfactory way using the extended Faber-Ziman formula with phase shifts depending on the energy. A very good agreement with the experiment is obtained, for resistivity, by using the Esposito procedure [19]. The energy dependence cannot be neglected in the thermoelectric power formula. The total treatment of the thermoelectric power (by numerical differentiation of the resistivity as a function of energy) leads to a considerable improvement of the theoretical results on the local calculations. Differences still exist between theory and experiment. They cannot be explained by the use of hard-sphere structure factors as has been noticed ([30,31]) for alloys near the melting point of the polyvalent metal. As spin contribution and DOS have been invoked to explain the Hall coefficient of bismuth, such effects may also play a role on the resistivity and thermopower of pure bismuth and bismuth rich alloys. The situation is different on the copper rich side where the d band determined with the Lloyd formula [32] has a too important effect on the thermopower.

References

[1] Ziman JM ;“ Electrons and phonons” version 1967, first published in1960, p 384.

[2] Ziman JM; “Principles of theory of solids” paperback second edition 1979, first published in 1964, p 230-232.

[3] Barnard RD; “Thermoelectricity in metals and alloys” 1972, p 62.

[4] Young WH; “Electrical transport properties”, Chapter 2.3, “Handbook of Themodynamic and Transport Properties of Alkali Metals” Blackwell Scientific Publications. Ohse W 1985.

[5] Sar F, Gasser J G ; Intermetallics 11 (2003) 1369-1376.

[6] Takeuchi S, and Murakami K.; Sci. Rep. Inst. Tohoku Univ. 25 (1974) 73-86.

[7] Chaïb C, Gasser J G, Hugel J, Roubi L; Physica B 252 (1998) 106-113.

[8] Ziman J M; - Phil. Mag., 6, (1961) 1013; -Adv. Phys., 13 (1964) 89.

[9] Faber T E and Ziman J. M ; Phil. Mag., 11 (1965) 153.

[10] Faber T E. “An introduction to the theory of liquid metals”. Cambridge, UK: Cambridge at the University Press (1972).

[11] Aschroft N W and Langreth D C ; Phys. Rev. 156 (1967) 685.

[12] Isherwood SP, Orton BR; Phil. Mag. 17 (1968) 561.

[13] Waseda Y;”The Struct. Of Non-Crystal. Material, Liquid and Amorphous Solids”. 1980.

[14] Sar F, Mhiaoui S, Gasser J G ; Journal of Non-Crystalline Solids 353 (2007) 3622-3627.

[15] Gasser J G ; J. Phys.: Condens. Matter 20 (2008) 114103.

[16] Mattheis L F ; Phys. Rev.133A, 1399 (1964).

[17] Mukhopadhyay G, Jain A and Ratti V K ; Solid State Com., (1973) 1623.

[18] Slater J C ; Phys. Rev., 81 (1951) 385.

[19] Esposito J C, Ehrenreich H and Gellat C D ; Phys. Rev. B, 18 (1978) 3913.

[20] Kreichgauer, Jaeger ; Ann. Phys. 47 (1892) 513.

[21] Roberts R B, Righini F. and Compton R.C.; Phil. Mag., B52 (1985) 114.

[22] Indlekofer G ; Thesis, “Systematics in the electronic structure of polyvalent liquid metals determined by electron spectroscopy” University of Basel (1987).

[23] Indlekofer G, Oelhafen P, Lapka R and Güntherodt H J. Z für Physikalische Chemie Neue Folge 157 S (1988) 465.

[24] Hafner J, Jank W; Phys. Rev. B, 45 (1992) 2739.

[25] Shiota I, Tamaki S; J. Phys. F. 7 (1977) 2361.

[26] Takeuchi S, Murakami K; SCI. REP. RITU, 25 (1974) 2-3.

[27] Lee D N and Lichter B. chap 3 of “Liquid Metals” edited by Sylvan Z Beer; Marcel Dekker Inc. New York (1972).

[28] Enderby JE , Chapter 14, “Liquid Metals”; Beer SZ (1972) p 611.

[29] Ballentine LE, Huberman M; J. Phys. C 10 (1977) 4991.

[30] Chaïb C and Gasser J G ; Zeitschrift Für Physikalische Chemie Neue Folge, Bd.156, (1988) 483-487.

[31] Gasser J G, Mayoufi M, Kleim R and Bellissent M. C.; J. Non. Cryst. Solid, , 117-118 (1990) 383.

[32] Lloyd P 1969 “Electrons in Metals and Multiple Scattering Theory” University of Bristol unpublished notes 1972 Adv. Phys. 21 p 69-142.

Captions

Table 1: Parameters used for the calculation using Esposito's procedure for pure copper and bismuth (with valence 3 and 5). Experimental and calculated resistivities, Seebeck coefficients and thermal conductivities.

Table 2: Coefficients of the least squares fit on the resistivity of liquid Cu_xBi_{1-x} alloys: $\rho = a_o + a_1 T + a_2 T^2$. ($\rho$ in $\mu\Omega.cm$ and T in Celsius).

Table 3: Coefficients of the least squares fit on the absolute thermopower of liquid Cu_xBi_{1-x} alloys: $S = b_0 + b_1 T + b_2 T^2$. ($S$ in $\mu V.K^{-1}$ and T in Celsius).

Figure 1: Experimental resistivity of pure liquid bismuth versus temperature.

Figure 2: Experimental absolute thermoelectric power of pure liquid bismuth versus temperature.

Figure 3: Energy dependence of the electrical resistivity for liquid bismuth. The Fermi energy with Z=3 and Z=5 is indicated.

Figure 4: Energy dependence of the thermopower for liquid bismuth. Local approximation (open circles) and full energy dependent calculation (full circles). The Fermi energy with Z=3 and Z=5 is indicated.

Figure 5: Energy dependence of phase shifts for liquid bismuth. The Fermi energy with Z=3 and Z=5 is indicated.

Figure 6: Experimental and theoretical density of states of liquid bismuth.

Figure 7: Experimental electrical resistivity of liquid Cu_xBi_{1-x} as function of temperature for different concentration.

Figure 8: Absolute thermoelectric power of liquid Cu_x-Bi_{1-x} as function of temperature for different concentration.

Figure 9: Thermal conductivity of liquid Cu_xBi_{1-x} as function of temperature for different concentration.

Figure 10: Resistivity of liquid copper-bismuth alloys as function of concentration at 1100°C.

Figure 11: Absolute thermoelectric power of liquid copper-bismuth as function of concentration at 1100°C.

Figure 12: Thermal conductivity as function of concentration deduced by equation (3a) either from experimental resistivity and thermopower or from Faber-Ziman calculated ones.

Metal	Copper at 1150°C	Trivalent bismuth at 950°C	Pentavalent bismuth at 950°C
Valency Z	1	3	5
Number of conduction electrons N_C	0.91	2.50	4.60
E_F (Ry)	0.45	0.44	0.66
$\eta_0(E_F)$	-0.280	-2.150	-2.460
$\eta_1(E_F)$	-0.011	0.960	0.990
$\eta_2(E_F)$	0.103	0.020	0.050
$\rho_{cal}(\mu\Omega.cm)$	8.5	161.9	74.9
$\rho_{exp}(\mu\Omega.cm)$	21.8	163.6	163.6
$S_{local}(\mu V/K)$	18.1	18.3	7.50
$S(\mu V/K)$	41.2	-8.30	-6.60
$S_{exp}(\mu V/K)$	17.8	-1.77	-1.77
$\lambda_{exp}(W/m.K)$	155.4	18.3	18.3
$\lambda_{cal}(W/m.K)$	371.15	20.69	-

Parameters used for the calculation using Esposito's procedure for pure copper and bismuth (with valence 3 and 5). Experimental and calculated resistivities, Seebeck coefficients and thermal conductivities.
209x297mm (600 x 600 DPI)

$Cu_x - Bi_{1-x}$	a_o	$a_1.10^3$	$a_2.10^5$
x=1	1.113	27.65	-0.816
x=0.95	-56.320	172.43	-7,423
x=0.90	-80.166	243.84	-10.166
x=0.80	98.016	-28.19	2.354
x=0.70	106.524	-7.27	1.507
x=0.60	116.875	8.86	1.123
x=0.50	137.527	-15.80	2.379
x=0.40	117.984	27.24	0.412
x=0.30	127.337	8.97	1.731
x=0.20	125.621	14.88	1.589
x=0.10	121.908	25.96	1.334
x=0	113.198	50.18	0.326

Coefficients of the least squares fit on the resistivity of liquid $Cu_x Bi_{(1-x)}$ alloys: $\rho = a_0 + a_1T + a_2T^2$.
(ρ in $\mu\Omega$cm and T in Celsius).
209x297mm (600 x 600 DPI)

$Cu_x - Bi_{1-x}$	b_0	$b_1.10^3$	$b_2.10^6$
x=1	23.224	-4.590	-
x=0.95	6.827	-1.78	-
x=0.90	5.081	-2.490	-
x=0.80	3.603	-2.180	-
x=0.70	1.421	-0.20514	-
x=0.60	0.287	0.70832	-
x=0.50	-0.077	0.50213	-
x=0.40	-0.227	-0.01424	-
x=0.30	-0.298	-0.48576	-
x=0.20	-0.163	-1.03	-
x=0.10	0.033	-1.73	-
x=0	-0.952	0.683	-1.490

Coefficients of the least squares fit on the absolute thermopower of liquid $Cu_x Bi_{(1-x)}$ alloys: $S = b_0 + b_1T + b_2T^2$. (S in μ V K^{-1} and T in Celsius).
209x297mm (600 x 600 DPI)

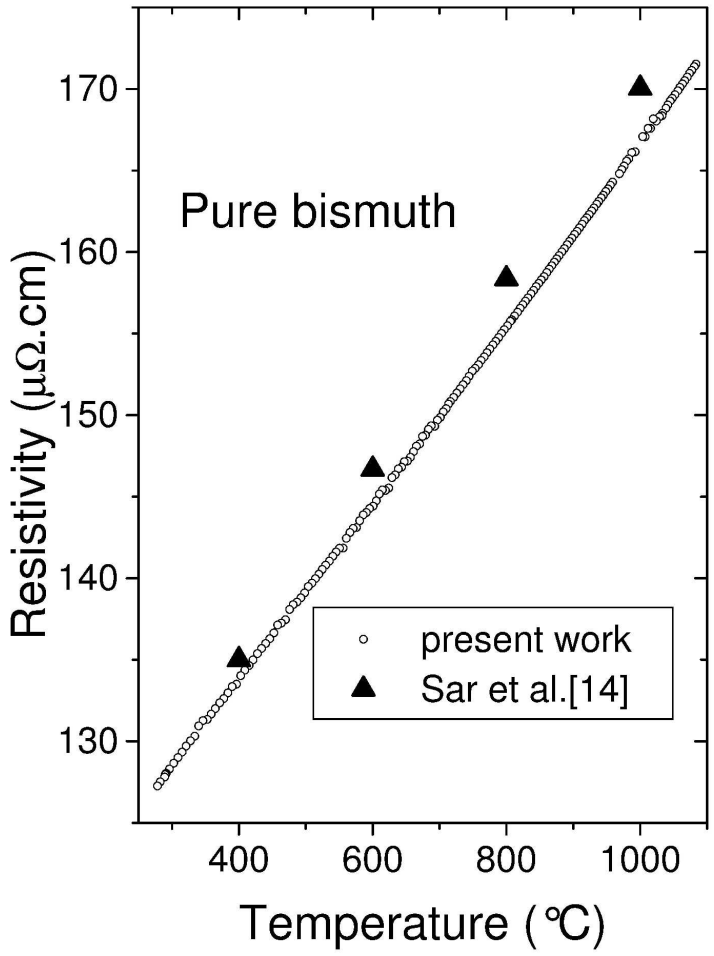

209x297mm (600 x 600 DPI)

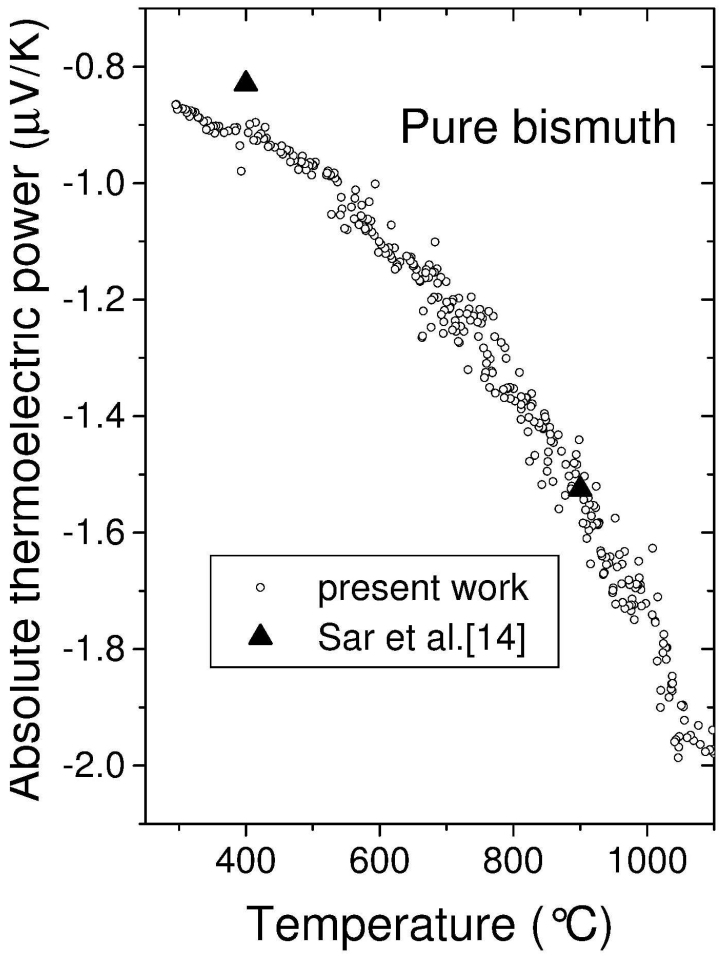

209x297mm (600 x 600 DPI)

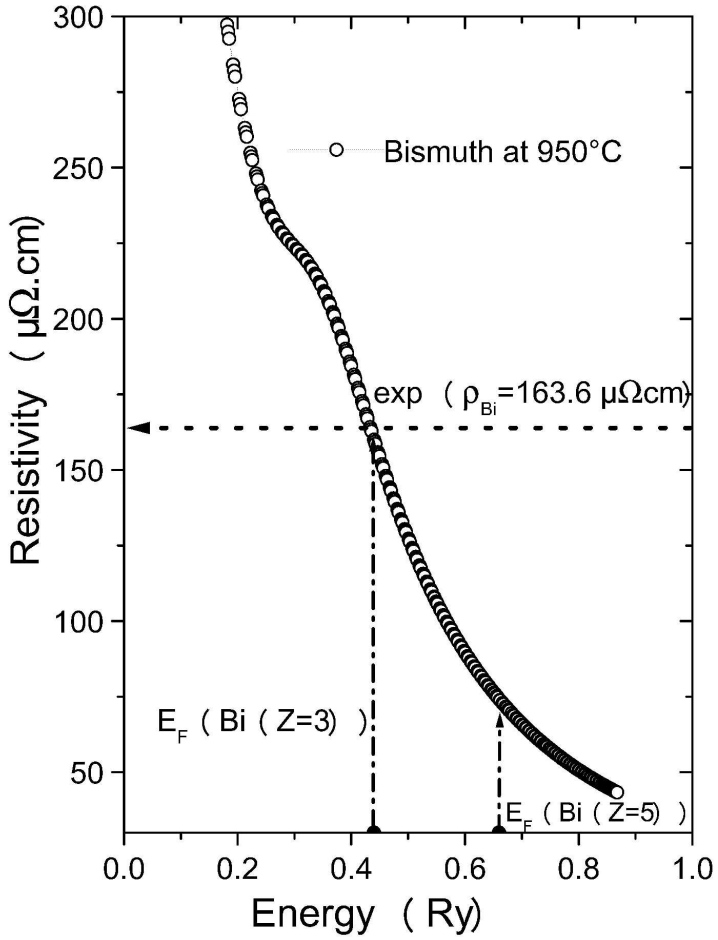

209x297mm (600 x 600 DPI)

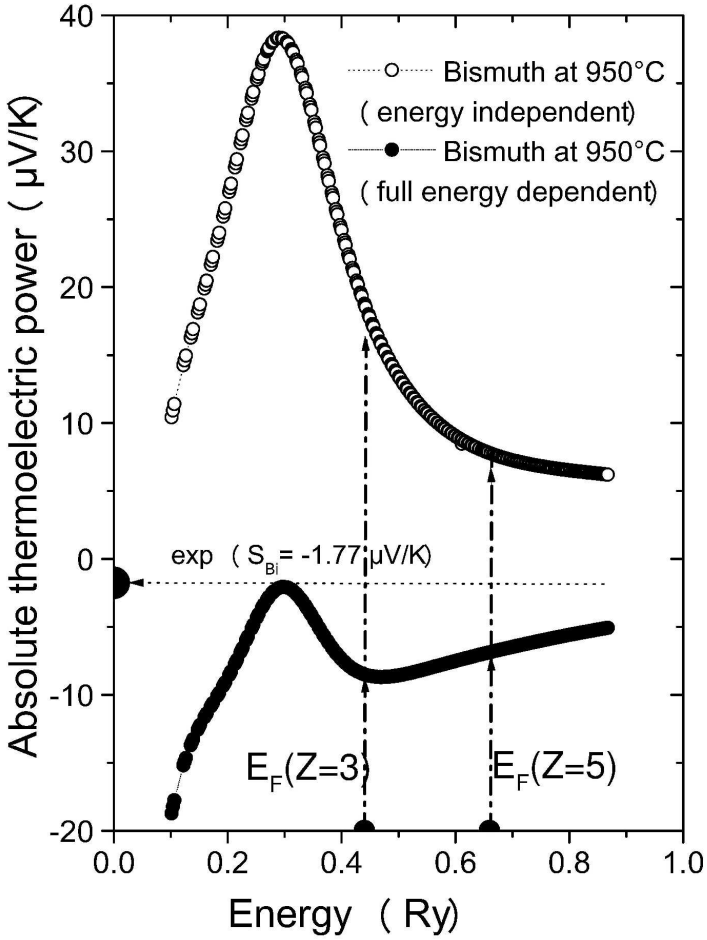

209x297mm (600 x 600 DPI)

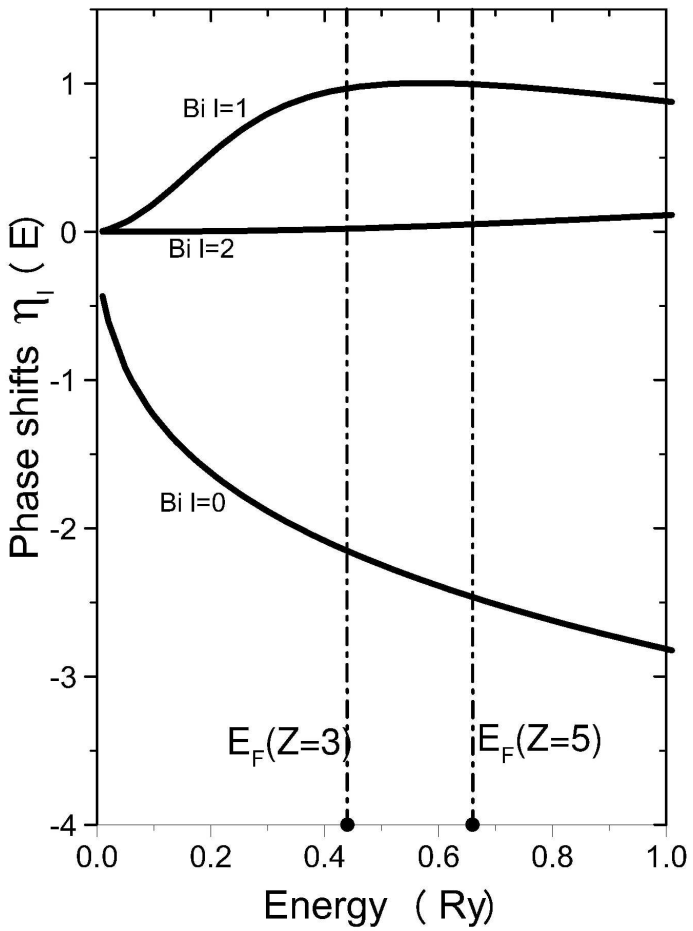

209x297mm (600 x 600 DPI)

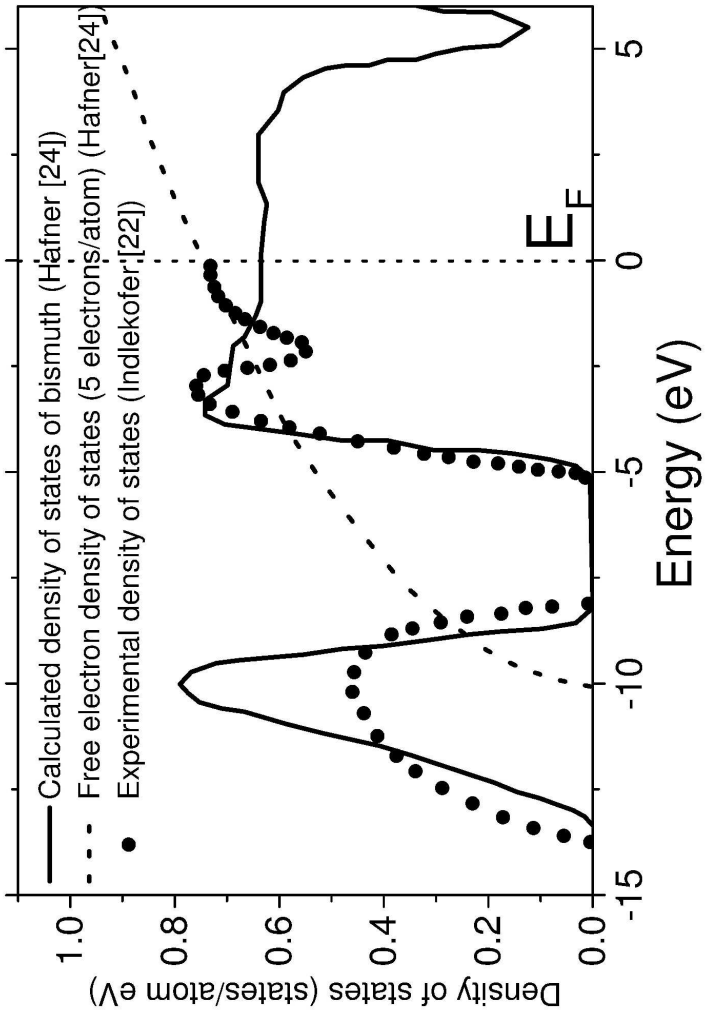

209x297mm (600 x 600 DPI)

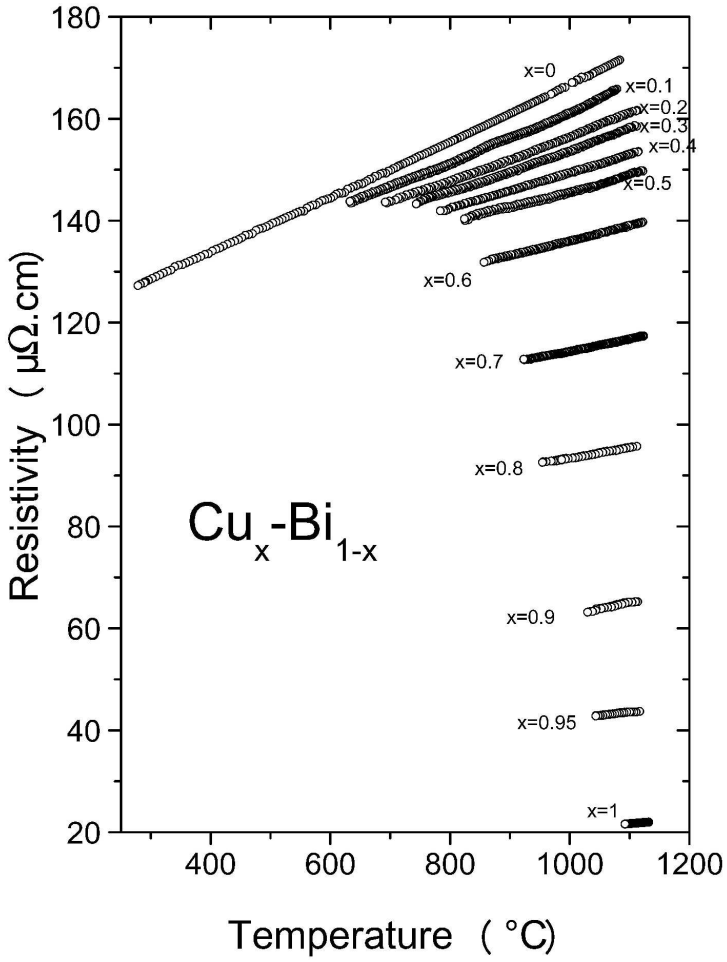

209x297mm (600 x 600 DPI)

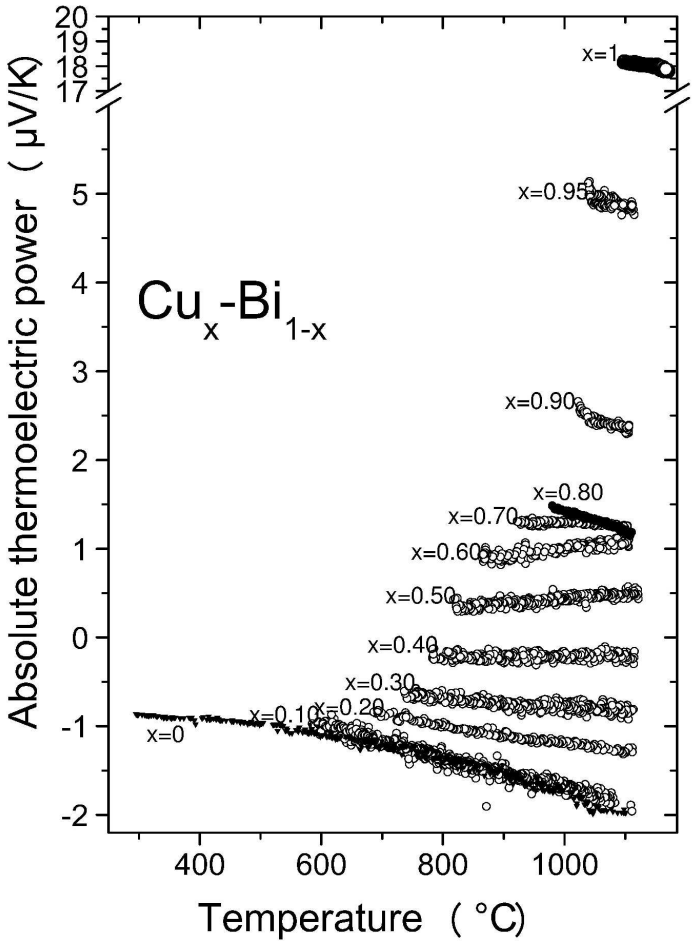

209x297mm (600 x 600 DPI)

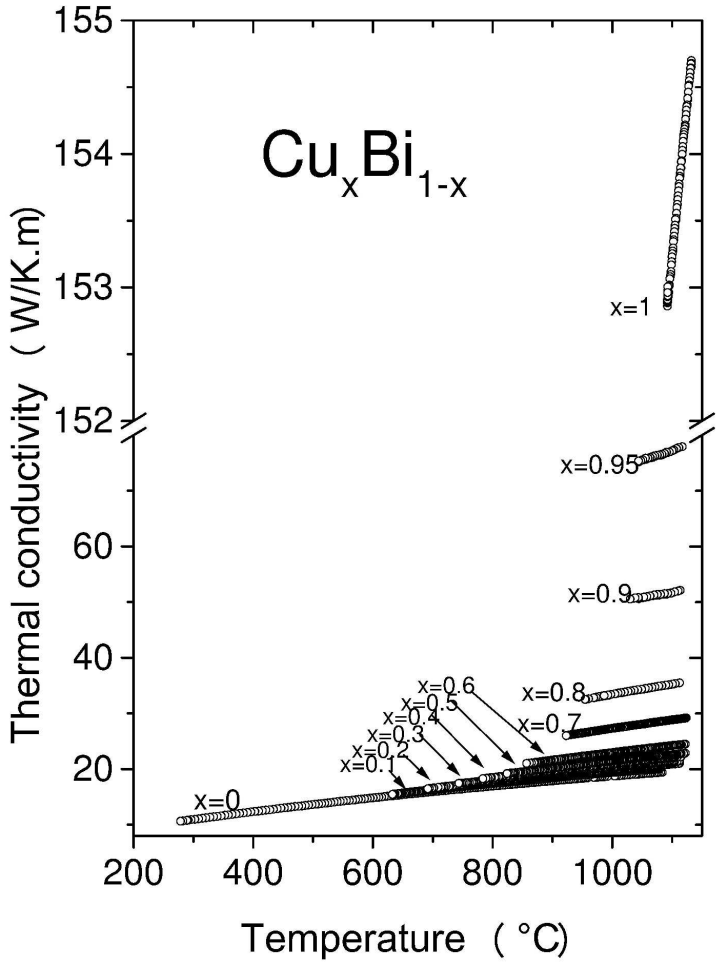

209x297mm (600 x 600 DPI)

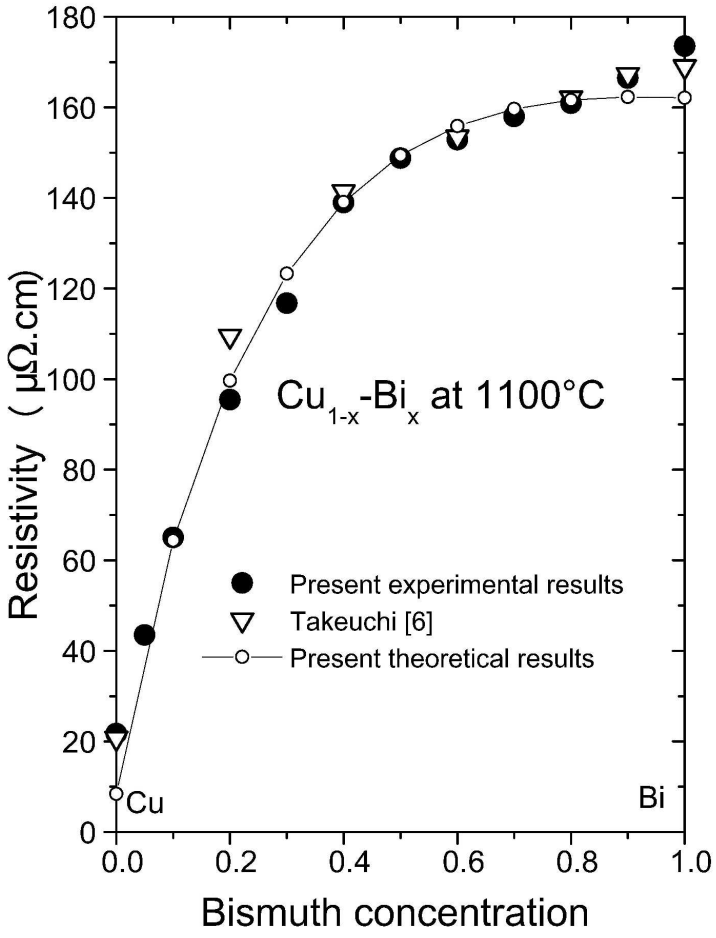

209x297mm (600 x 600 DPI)

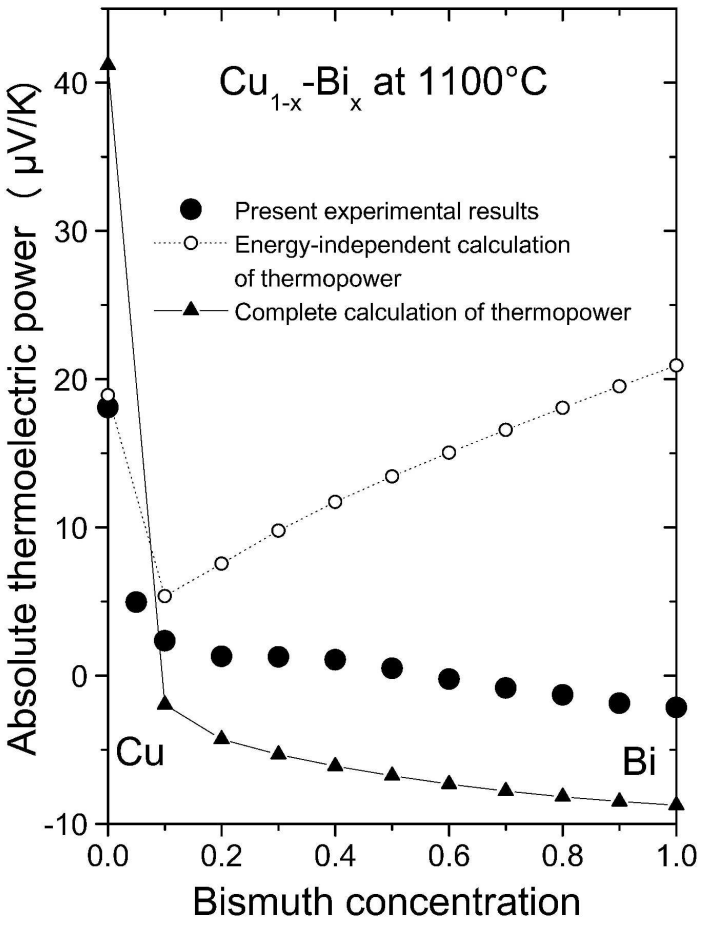

209x297mm (600 x 600 DPI)

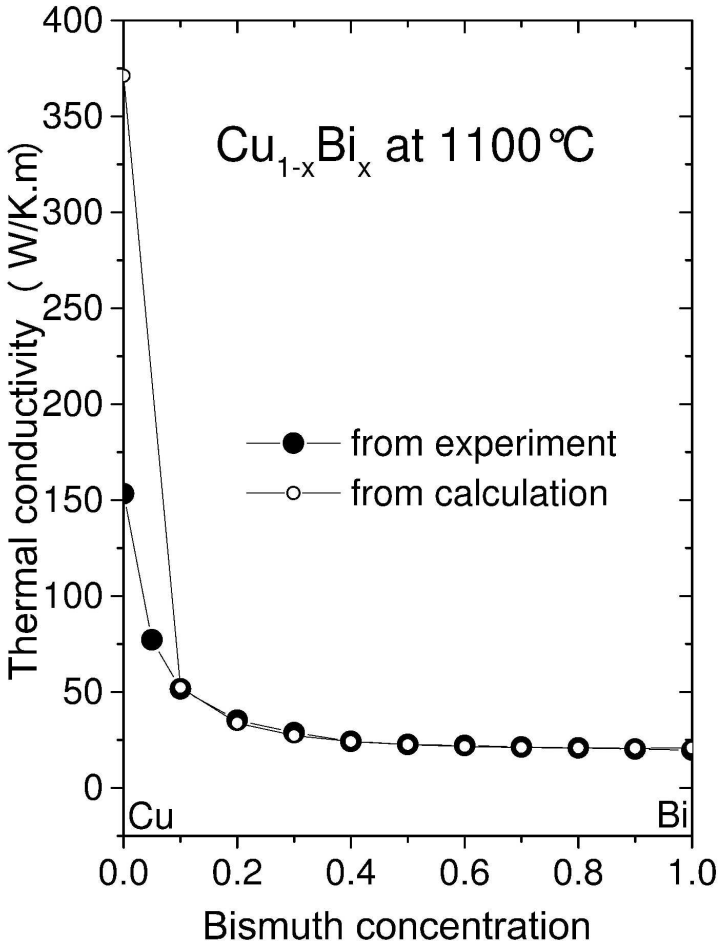

209x297mm (600 x 600 DPI)